Fully automatic segmentation of stained histological cuts

Jiří BOROVEC *

Center for Machine Perception, Faculty of Electrical Engineering,
Czech Technical University in Prague, Czech Republic

jiri.borovec@fel.cvut.cz

Abstract. *The paper describes an automatic unsupervised segmentation of stained histological sections, which would be suitable for further registration of series of stained consecutive histological cuts. We combine some already existing methods – Gaussian Mixture model above colour histogram, superpixels to increase the robustness and speed and the Graph Cut method to obtain compact segmentation. We show the experimental results and segmentation precision on both synthetic and real histological images. For synthetic images we reach mean classification error for* 4*-class segmentation of about* 3%*. The unsupervised segmentation on real images shows us always reasonable object, which is important for future segmentation-based registration.*

Keywords

Superpixel, segmentation, GMM, Graph Cut, superpixels, histological sections, stains.

1. Introduction

The technologies for capturing microscopy images (see Fig.1a,b,c) of nowadays machines are capable to capture very large images with high resolution. Typically the coloured histological images we work with have mean image size of around 40.000×40.000 pixels. In this paper we deal with series of stained histological images stained by various dyes, such as H&E, Pro-SPC, CC10, Ki67, CD31, etc.

Image segmentation as well as registration are frequently used in medical imaging. For the last decades the image registration is rapidly growing and many interesting methods were developed [2] for various applications such as microscopy, US, MRI and CT images. We found that the main standard feature and intensity based registration techniques fail on large stained histological images. In feature based registration, finding the correct match between detected features is hard because of repetitive texture (in detail). The intensity based registration for such large images is very time demanding without any special sampling strategy which could be more sensitive to falling into local minima. In general segmentation as well as registration for such large images is very hard to use because of time efficiency and available computation resources.

We assume that if we are able to segment the images into a few classes we would not lose much spatial information comparing to the original images. Furthermore, the registration on the segmented images would be more robust than the state-of-the-art methods and also faster when using simple criteria. The aim of this paper is develop a fully automatic segmentation estimating a few compact classes which could appear in whole series of histological cuts using other segmentation techniques. We assume the biological meaning of the segmented objects/regions is not very important.

Segmentation has been used in medical imaging for a long time and many segmentation techniques were published [3, 4, 5]. In the last few years several interesting articles about semi-automatic [6] and automatic [7, 8, 9, 10] segmentation of histological images were introduced.

Image segmentation models such as Bayesian classification together with Markov Random Field (MRF) were first introduced in [11]. This approach was recently applied on histological images as a supervised image segmentation [6] which uses the Metropolis algorithm. Furthermore for large images Monaco proposed a growing region procedure to decrease dimensionality and extract more robust features and then he optimised created MRF using Dhull algorithm [10].

This developed segmentation takes inspiration from both methods [10, 6]. We use Bayesian and MRF segmentation model. The proposed pipeline is: (1) SLIC superpixel segmentaion [12] to decrease the complexity and estimate reasonable region; (2) computing colour descriptors on extracted superpixels; (3) unsupervised learning of the probabilistic models of expected classes using the Expectation-Maximisation (EM) algorithm [13] initialised by K-means [14] for Gaussian mixture models (GMM) [15]; (4) Graph Cut [16] segmentation to obtain compact segmentation. Another reason for using superpixels is the very extreme time complexity for applying Graph Cut segmentation [17] on pixel grid for large images (more than $5.000.000$ pixels).

For experimental evaluation we created a dataset of synthetic images which simulates the structures and colours

∗ This paper is partial short-cut and extension of [1].

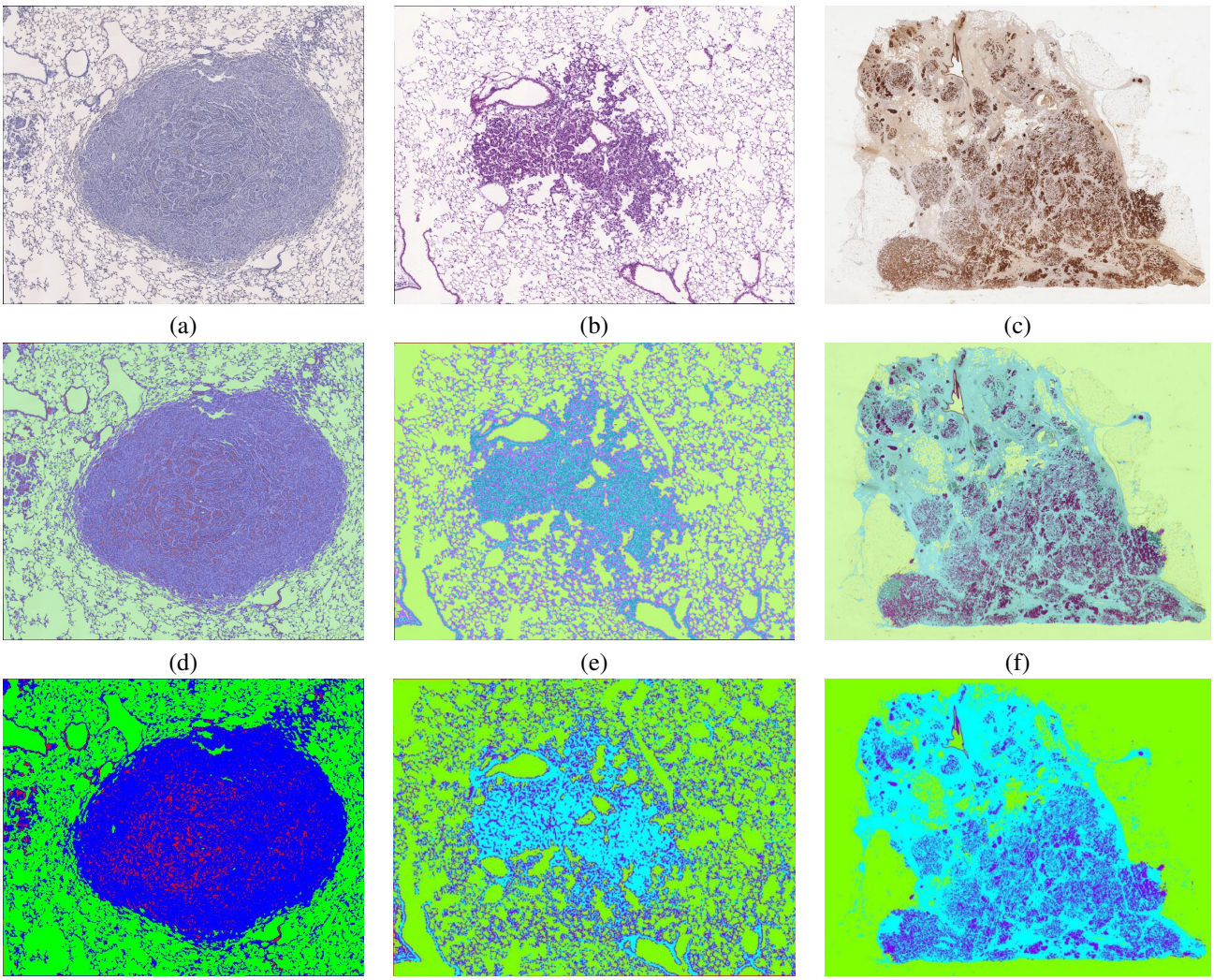

Fig. 1: Examples of stained histological sections are presented in (a,b,c). The two lesions (a,b) are coloured by dyes CD31 and H&E respectively. The Human breast (c) is stained by Cytokeratin. The bottom row (g,h,i) contains the segmentations of images shown in the top row (a,b,c) in the same order. The optical overlap between the original image and its segmentation is presented in middle row (d,e,f).

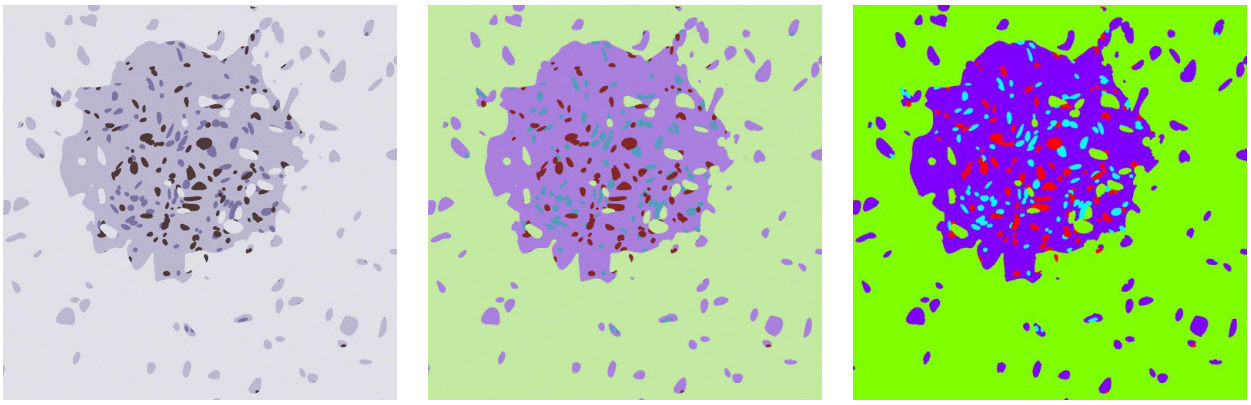

Fig. 2: Examples of synthetic image simulating real long-lesion (a) which represents the CD31 dye. For better visualisation we used transparent overlap (b) of the original image (a) and its segmentation (c).

measured on real lesions (see Fig.2). Further we show the segmentation result on the real stained histological images (see Fig.1). We create manual segmentation of this images using a semi-automatic method - Weka segmentation [18] implemented in ImageJ[1].

The paper structure is the following: in Sec.2 we formulate the segmentation problem, show the Bayesian segmentation model and colour descriptors extraction on estimated superpixels; in Sec.3.1 we introduce the synthetic and real images we work with; followed by experiments on these images in Sec.3 and finally in Sec.4 we evaluate the segmentation method for registration.

2. Methodology

The input of the segmentation algorithm is a 2D colour image of a colour histological cut. We want to segment into a small number of compact classes where spatially close pixels should be likely to belong to the same class.

More formally, let us define a set of integer pixel coordinates $\Omega \subseteq \mathbb{Z}^d$ where d is the dimensionality. For 2D images $d = 2$ and we assume that Ω is a hyperinterval, $\Omega = [1, \ldots, n_x] \times [1, \ldots, n_y]$. The image is represented as a function $X : \Omega \to \mathbb{R}^m$ where each pixel is a vector with dimension m, typically for colour (RGB) images $m = 3$. We use a superpixel segmentation (labelling) function S which classifies pixels by colour intensities and distances between pixels, assigning all pixels in Ω to a superpixel $\Omega_s \in \Omega$. We also define a finite set of labels $\mathbb{L}$ and a segmentation function Y_s, which assigns a label $k \in \mathbb{L}$ to each superpixel $Y_s : \Omega_s \to \mathbb{L}$. Then all pixels in a superpixel Ω_s have the same label k so the labelling function Y label also all pixels $Y : \Omega \to \mathbb{L}$.

2.1. Class estimation

We estimate the class $y_i = Y(i)$ for each image pixel $x_i = X(i)$ where the $i \in \Omega$ represents the pixel coordinate, by calculating the maximum a posteriori (MAP) estimate $P(Y|X)$. Let us define the final class estimation (segmentation) Y^* as

$$Y^* = \arg\max_Y \ P(Y|X) \tag{1}$$

Applying Bayes' theorem [19] we get

$$Y^* = \arg\max_Y \ \frac{p(X|Y) \cdot P(Y)}{p(X)} \tag{2}$$

where $p(X)$ is the marginal probability density function (pdf) of observation X, $P(Y)$ is the probability of a specific segmentation (of all pixels) regardless of the measurement and $p(X|Y)$ is the conditional density of X given Y.

[1] http://rsb.info.nih.gov/ij/

We can omit $p(X)$ from the formulation because it is constant for a given image X. To express the spatial model dependence we propose to use Markov fields. Then the term $P(Y)$ can be written as

$$P(Y) = \prod_i h(y_i) \cdot \prod_{\substack{i \neq j \\ d(i,j) \leq 1}} R(y_i, y_j) \tag{3}$$

The first term $h : \mathbb{L} \to \mathbb{R}$ is the prior probability of each class independent of the position. The second term $R(y_i, y_j)$ describes the relation between classes of neighbourhood pixels. The pixel neighbouring is formulated by the following rule $i \neq j$; $d(i,j) \leq 1$ where $d(i,j)$ is the l_1 distance between two pixel coordinates i, j.

Because pixels are conditionally independent given Y, the equation can be then written as

$$Y^* = \arg\max_Y \prod_i (p(x_i|y_i) \cdot h(y_i)) \cdot \prod_{\substack{i \neq j \\ d(i,j) \leq 1}} R(y_i, y_j) \tag{4}$$

We solve this problem by the Graph Cut method. We take the negative logarithm of eq.(4) to obtain the formula

$$Y^* = \arg\min_Y \ -\sum_i \log\left(p(x_i|y_i) \cdot h(y_i)\right) - \sum_{\substack{i \neq j \\ d(i,j) \leq 1}} \log R(y_i, y_j) \tag{5}$$

For simplification we define function B as

$$B(k,l) = -\log R(k,l) \tag{6}$$

where k, l are labels, i.e. $k, l \in \mathbb{L}$.

A commonly used Potts model corresponds to

$$B(k,l) = \beta \cdot \delta_{k,l} + C = \beta \cdot [\![k \neq l]\!] + C \tag{7}$$

where the Kronecker delta $[\![k \neq l]\!]$ can be represented as a square matrix with zeros on the main diagonal and ones otherwise. The β is a regularisation coefficient. Because the additive constant C does not effect Y^*, we omit it.

Let us further define

$$U(x_q, y_q) = -\log(p(x_q|y_q) \cdot h(y_q)) \tag{8}$$

Rewriting eq.(5) we obtain the following minimisation problem

$$Y^* = \arg\min_Y \ \sum_i U(x_i, y_i) + \sum_{\substack{i \neq j \\ d(i,j) \leq 1}} B(y_i, y_j) \tag{9}$$

The problem formulation by eq. (9) can be solved by Graph Cut. The unary term $U(x_i, y_i)$ represents the measurements and an a priori class probability. The binary potential $B(y_i, y_j)$ leads to spatial regularisation.

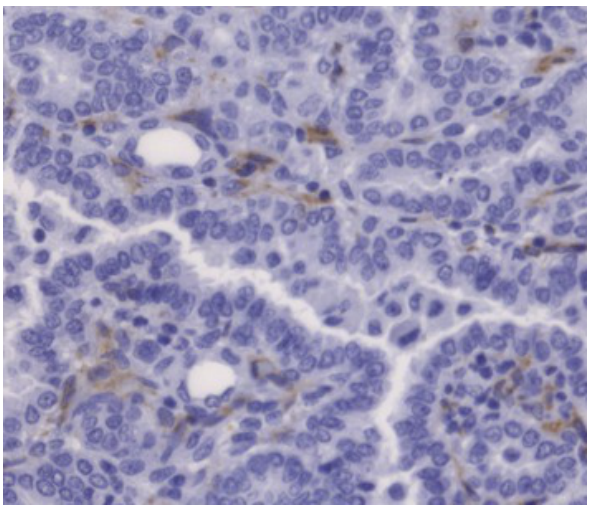

(a)

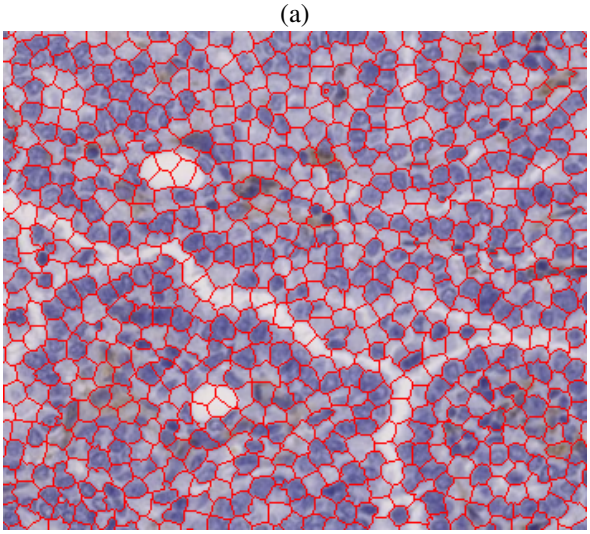

(b)

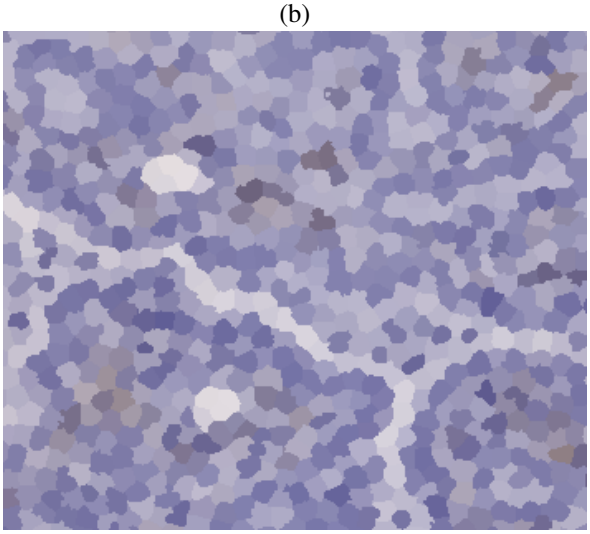

(c)

Fig. 3: The SLIC superpixel segmentation in detail (b) for the original colour histological image (a) presented in Fig.1a). The initial segmentation grid was chosen optimally, because the estimated superpixels nicely fit to nuclei, the smallest object we want distinguish. Then computing the mean colour for all superpixels (c) we do not lose much spatial information comparing to the original image (a).

2.2. Superpixels and descriptors

We have to specify the probability model $p(x_i|y_i)$ used in eq.(8). In the previous section we defined a colour descriptor for each superpixel s_i formed by RGB colour components. We can use these colour descriptors to create the probability model $p(x_i|y_i)$.

For the SLIC segmentation the most sensitive parameter is the initial grid size for these estimated superpixels. According to [16] the size of this grid has to be smaller than the size of the smallest detail in image that we want discriminate. The resolution level that we are interested in segmentation of the real images is equal to separating individual nuclei in the histological images.

After the images are segmented using SLIC superpixels, we compute descriptors for each superpixel. Other state-of-the-art methods frequently use colour [10] and texture [20, 6] descriptors or both [15]. We found that the colour descriptors are sufficient, because relatively small superpixels do not cover much texture information. We compute the superpixel colour descriptors as a mean colour intensity over all pixels belongs to the superpixel

$$s_j = \frac{1}{\|\Omega_j\|} \cdot \sum_{i \in \Omega_j} x_i \tag{10}$$

and then we create the probability model $p(s_i|y_i)$ from these extracted features.

2.3. Multi-class modeling

We define a set of models with parameters $\Theta = (\theta_1, \ldots, \theta_{\|\mathbb{L}\|})$ of the class densities $p(\boldsymbol{s}_i|y_i = k)$. The model of a class k is characterised by parameters θ_k where $k \in \mathbb{L}$. For simplification we choose a Gaussian model so the model parameters are $\theta_k = (\boldsymbol{\mu}_k, \boldsymbol{\Sigma}_k)$, where $\boldsymbol{\mu} \in \mathbb{R}^m$ is a vector of means and $\boldsymbol{\Sigma} \in \mathbb{R}^{m \times m}$ is a covariance matrix. The pdf is

$$p(\boldsymbol{s}_i|\theta_k) = N(\boldsymbol{s}_i, \boldsymbol{\mu}_k, \boldsymbol{\Sigma}_k) \tag{11}$$

We estimate $\boldsymbol{\mu}_k$ and $\boldsymbol{\Sigma}_k$ using the EM algorithm[13] which also estimates the a priori probability $h(k)$ of each class. The EM algorithmconverges only to local minima, so the convergence to the global optimum also depends on the initialisation. For initialisation we take randomly $\|\mathbb{L}\|$ samples from the whole set. Then to avoid initialisation leading to local minima we compute a minimal number W of random initialisations to have at least one initialisation close to the expected true estimation. The W is defined as the number of randomly taken initial samples from same expected clusters

$$W = 1 + \sum_{i \in \mathbb{L}} (M - i + 1) \cdot \frac{M!}{i! \cdot (M - i)!} \Bigg|_{M = \|\mathbb{L}\|} \tag{12}$$

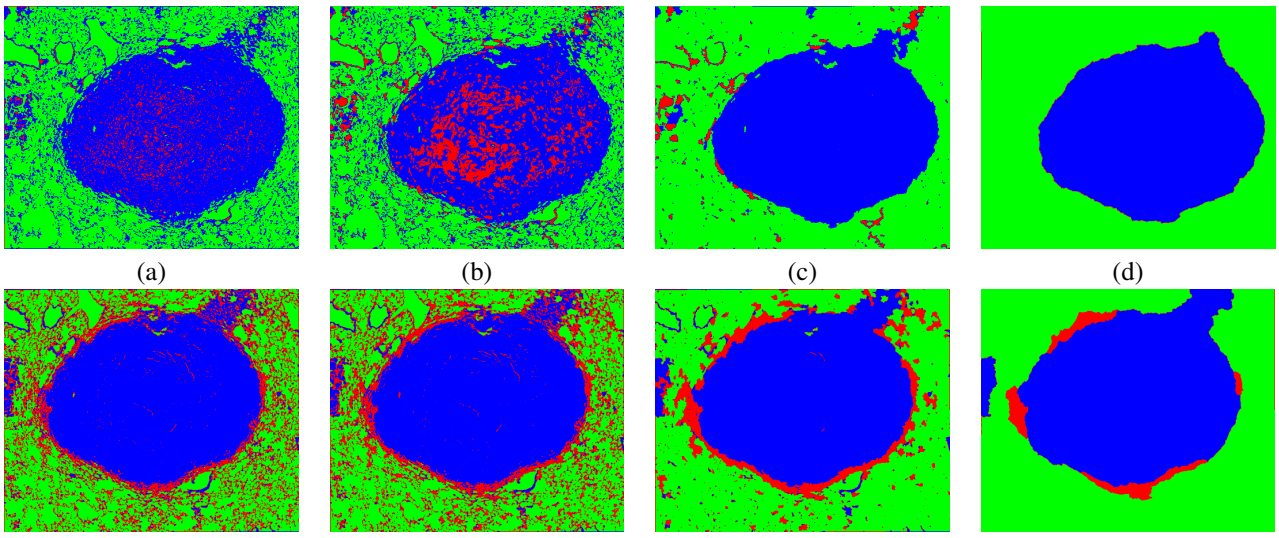

Fig. 4: Illustration of how the chosen Graph Cut regularisation influence the segmentation compactness and also the level of detail. We estimated one classification model and segmented this model by Graph Cut with various regularisation constants $[1000, 10000, 30000, 100000]$ shown in rows (a,b,c,d) and (e,f,g,h) respectively. The two different stained lesions (CD31 in the top row and H&E in bottom row) for the same regularisation constant containa similar amount of detail.

3. Experiments

In this section, we introduce both, the created synthetic and the real images we work with (see Fig.1). Then we present the experimentally measured precision of our segmentation method and illustrate the dependency of chosen regulation constant in Graph Cut to the segmentation consistency (see Fig.4).

According to the biological meaning of the real histological images we fix the number of estimated classes $M = \|\mathbb{L}\| = 4$ for all images.

3.1. Material

We will evaluate both algorithm on synthetic images and also real histological cuts of lesion. First we present four synthetic datasets each consisting of 99 image pairs with various transformations between them. Then we introduce two consecutive sequences of the lesions coloured by 5 different stains each.

Synthetic images. We create a compact 4-class segmentation. Then, we assign to each class a colour such that all created images X have the same colours representation as one of possible stains in real histological images. To get texture pattern we add 5% white Gaussian noise. The size of these images are 1600×1600 pixels.

Real images. We have used material extracted from long-term urethane. For now, two nodules (adenoma or adenocarcinomas) were acquired with a Zeiss Axio Imager M1 microscope with a 40x dry objective. Consecutive sections were stained with: H&E (Hematoxylin and Eosin), Pro-SPC (pulmonary pro-surfactant protein C segregated by type 2 pneumocytes), CC10 (Clara Cells 10 protein), Ki67 (cancer antign that is found in growing dividing cells but is absent in the resting phase of cell growth), CD31 (Platelet endothelial cell adhesion molecule-1. It is a protein expressed at high levels on early and mature endothelial cells, platelets, and most leukocyte sub-populations).

For evaluation, an expert created reference segmentations by Weka segmentation plugin [18] implemented in ImageJ. He segmented 4 biological structures in each image. Because of implementation and resources limitation we were not able to segment whole images but only individual parts and then we compose them together.

3.2. Assignment problem

The segmentation of each image is made independently so that identical objects in two different images might be denoted by different labels k. To evaluate our segmentation we need to find a correspondence between the class labels in both reference and estimated segmentation.

Let us define the consistency error

$$E(a,b) = \frac{1}{\|\Omega\|} \cdot \sum_{i \in \Omega} [\![y_i^a \neq y_i^b]\!] \tag{13}$$

where the $a, b \in \mathbb{L}$ are classes in two different images A and B respectively. We use the Hungarian algorithm [21] which

dataset	relative error	
	mean	std
Synthetic	3.19%	4.88%
Lesions	24.6%	5.8%

Tab. 1: Relative classification error for both synthetic and real images. For the synthetic images where the structures were quite clearly given segmentation works nice. The second case - real images, the segmentation does not much well section by a biological meaning.

using the defined criterion $E(a, b)$ finds one-to-one assignment between two segmented images A and B. Then we define a classification error ϵ as the relative number of unequally labelled pixels in both reference and estimated segmentations

$$\epsilon = \frac{1}{\|\Omega\|} \cdot \sum_{i \in \Omega} [\![y_i^R \neq y_i^*]\!] \tag{14}$$

where the Y^R and Y^* are reference and estimated segmentation respectively.

3.3. Synthetic images

Firstly we validate our segmentation on synthetic images (see Fig.2) described in Sec.3.1. These images have a precise given number and mean colour of all classes by the structure they simulate. We run the segmentation on all 99 images in the dataset. The mean error of misclassified pixels between reference and obtain segmentation was 3.19% (see Tab.1).

3.4. Real images

We have the manual segmentation of several lung-lesion, each coloured by 5 different dyes presented in Sec.3.1. We ran our segmentation on the real images. The results for both sets of real images are presented in Tab.1. We consider this comparison only as illustrative because our method does not aim to segment sections with an specific biological meaning as the expert did. Moreover we do not specify the structures our segmentation should look for.

According to the segmentation for registration we demand estimation of compact reasonable segments. Moreover we would like to influence number of detail in the segmented images. We show in Fig.4 two segmentations of consecutive cuts (they are supposed to be the same) coloured by different dyes. Both segmentations are very similar by using the same regularisation constant (Graph Cut).

4. Conclusion and discussion

We have presented a method for segmentation large images of colour histological sections using superpixel segmentation, colour descriptors, Gaussian model, EM and K-means algorithm and Graph Cut. We are able to segment really large images (size of around 40.000×40.000 pixels) while some other nowadays segmentations cannot do because of implementation and resources limitations.

Using synthetic images we proved the precision of our segmentation method. When segmenting real images without any a priori knowledge about segmenting images we can not expect equal segmentation as the expert does with a semi-automatic tool. On the other hand we show that our segmentation method does segmentation which would be very useful for the registration of stained histological sections. We also compare to other segmentation tools and conclude that we are able to segment whole large images.

Acknowledgements

Research described in the paper was supervised by doc. Jan Kybic, FEE CTU in Prague and supported by the Czech Science Foundation under the project P202/11/0111 and by the Grant Agency of the Czech Technical University in Prague under the grant SGS12/190/OHK3/3T/13.

References

[1] J. Borovec. Segmentation for registration of histological cuts. Technical report, CMP CTU, Prague, CZ, 2012.

[2] B. Zitova. Image registration methods: a survey. *Image and vision computing*, 21(11):977–1000, 2003.

[3] Dzung L Pham, Chenyang Xu, and Jerry L Prince. A Survey of Current Methods in Medical Image Segmentation. *In Annual Review of Biomedical Engineering*, 2:315–338, 2000.

[4] D.J. Withey and Z.J. Koles. Medical Image Segmentation: Methods and Software. In *Joint Meeting of the 6th International Symposium on Noninvasive Functional Source Imaging of the Brain and Heart and the International Conference on Functional Biomedical Imaging*, pages 140–143. Ieee, October 2007.

[5] A. Elnakib, G. Gimel'farb, J.S. Suri, and A. El-Baz. Medical Image Segmentation: A Brief Survey. In *Multi Modality State-of-the-Art Medical Image Segmentation and Registration Methodologies*, pages 1–39. Springer New York, 2011.

[6] Ching-Wei Wang, Dean Fennell, Ian Paul, Kienan Savage, and Peter Hamilton. Robust automated tumour segmentation on histological and immunohistochemical tissue images. *PloS One*, 6(2):e15818, January 2011.

[7] A. Hafiane, F. Bunyak, and K. Palaniappan. Evaluation of level set-based histology image segmentation using geometric region criteria. In *International Symposium on Biomedical Imaging, IEEE*, pages 1–4, 2009.

[8] Y. Peng, Y. Jiang, and L. Eisengart. Segmentation of prostatic glands in histology images. In *International Symposium on Biomedical Imaging, IEEE*, pages 2091–2094. Department of Radiology, the University of Chicago, IL 60637, USA, IEEE, 2011.

[9] Y. Peng, Y. Jiang, and L. Eisengart. Computer-aided identification of prostatic adenocarcinoma: Segmentation of glandular structures. *Journal of Pathology Informatics*, 2:33, January 2011.

[10] J.P. Monaco and J.E. Tomaszewski. High-throughput detection of prostate cancer in histological sections using probabilistic pairwise Markov models. *Medical Image Analysis*, 14(4):617–29, August 2010.

[11] M. Berthod, Z. Kato, S. Yu, and J. Zerubia. Bayesian image classification using Markov random fields. *Image and Vision Computing*, 14(4):285–295, 1996.

[12] R. Achanta and A. Shaji. SLIC Superpixels Compared to State-of-the-art Superpixel Methods. *Pattern Analysis and Machine Intelligence, IEEE*, 34(11):2274 – 2282, 2012.

[13] G. Xuan and W. Zhang. EM algorithms of Gaussian mixture model and hidden Markov model. *Image Processing, 2001.*, 1:145–148, 2001.

[14] J.A. Hartigan and M.A. Wong. Algorithm AS 136: A K-means clustering algorithm. *Journal of the Royal Statistical Society. Series C (Applied Statistics)*, 28(1):100–108, October 1979.

[15] H. Permuter, J. Francos, and I. Jermyn. A study of Gaussian mixture models of color and texture features for image classification and segmentation. *Pattern Recognition*, 39(4):695–706, April 2006.

[16] A. Lucchi, K. Smith, and R. Achanta. Supervoxel-Based Segmentation of Mitochondria in EM Image Stacks With Learned Shape Features. *Medical Imaging, IEEE*, 31(2):474 – 486, 2012.

[17] Y. Boykov and O. Veksler. Fast approximate energy minimization via graph cuts. *Pattern Analysis and Machine Intelligence, IEEE*, 23(11):1222–1239, 2001.

[18] M. Hall, E. Frank, and G. Holmes. The WEKA data mining software: an update. *SIGKDD Explorations*, 11(1), 2009.

[19] R.O. Duda, P.E. Hart, and D.G. Stork. *Pattern Classification and Scene Analysis*. John Wiley & Sons, 1973.

[20] M. Unser. Texture classification and segmentation using wavelet frames. *Image Processing, IEEE*, 4(11):1549–1560, 1995.

[21] H. W. Kuhn. The Hungarian method for the assignment problem. *Naval Research Logistics Quarterly*, 2(1-2):83–97, March 1955.

About Authors...

Jiří Borovec received a MSc double-degree from IUP System Intelligent on Universite Paul Sabatier, France, and Faculty of Mechatronics at Technical University of Liberec, Czech Republic. He is currently pursuing a PhD degree at Faculty of Electrical Engineering of the Czech Technical University in Prague. His research interests include image registration and segmentation of stained histological sections, medical imaging and robotic.